Molecular Therapy
Methods & Clinical Development
Original Article

Transient Chimeric Ad5/37 Fiber Enhances NK-92 Carrier Cell-Mediated Delivery of Oncolytic Adenovirus Type 5 to Tumor Cells

Jian Gao,[1] Wenli Zhang,[1] Kemal Mese,[1] Oskar Bunz,[1] Fengmin Lu,[2] and Anja Ehrhardt[1]

[1]Virology and Microbiology, Center for Biomedical Education and Research (ZBAF), Department of Human Medicine, Faculty of Health, Witten/Herdecke University, Witten, Germany; [2]State Key Laboratory of Natural and Biomimetic Drugs, Department of Microbiology & Infectious Disease Center, School of Basic Medical Sciences, Peking University Health Science Center, Beijing 100191, China

Methods for customizing and improving virus vector tropism are limited. In this study, we introduce a microRNA (miRNA)-regulated molecular method to enhance vector transduction without genome alteration. Based on the importance of adenovirus (Ad) vectors for cancer and gene treatment, we exemplified this technology for an Ad type 5 (Ad5) vector temporally carrying a knob from Ad37. We constructed a producer cell line stably expressing a fused Ad5/37 chimeric fiber comprising the Ad5 shaft-tail and the Ad37 knob and a miRNA inhibiting Ad5 knob expression (HEK293-Ad5/37-miRNA). The chimeric Ad5/37 vector resulted in enhanced transduction rates in Ad37 adequately and Ad5 poorly transduced cells. Particularly, encapsidation of the oncolytic Ad5-human telomerase reverse transcriptase (hTERT) vector genome into the chimeric Ad5/37 capsid showed efficient transduction of NK-92 carrier cells. These infected carrier cells then delivered the oncolytic vector to tumor cells, which resulted in enhanced Ad5-hTERT-mediated tumor cell killing. We show that this transiently capsid-modified chimeric vector carrying an Ad5 genome displayed higher transduction efficiencies of natural killer cell-derived NK-92 cells utilized as carriers in cancer immune therapy. In summary, transiently modified adenoviral vectors will have important implications for cancer and gene therapy.

INTRODUCTION

Adenoviral vectors combine several features, including infection into quiescent and dividing cells, a large cargo capacity, transduction of a broad variety of cell types, and a low risk of genotoxicity due to low integration rates into the host genome. In fact, 19.5% of vectors used in gene therapy clinical trials are based on adenovirus (Ad) (http://abedia.com/wiley/vectors.php), and various adenoviral vectors are emerging for preclinical and clinical gene therapeutic approaches, vaccination studies, and oncolytic virotherapy. More than 100 human Ad types have been identified and classified into seven species (A to G),[1,2] but historically most studies in basic and translational research were performed with Ad types 2 and 5. Ad5 vectors continue to receive considerable attention in laboratories and clinical trials, because they show efficient expression of exogenous genes and they can be amplified and purified at high titers. Cellular infection of Ad5 is mediated through the initial binding of the fiber knob domain to the coxsackie virus and Ad receptor (CAR) on the cell surface.[3–5] However, the low expression and even deficiency of Ad5 receptors on many cells render them refractory to Ad5 vector expression.[6] Therefore, extremely high viral titers for sufficient infection rates of target cells are required, resulting in dose-related toxicity and compromised therapeutic efficiency.[7–9]

To address this problem, the necessity to improve the transduction efficiencies of Ad5 vectors is becoming increasingly important to minimize adverse dose-dependent effects. Several optimizations were explored such as pseudotyped adenoviral vectors with a genetically modified capsid,[10–12] chemical modifications of the capsid proteins,[13–15] bispecific antibodies (Abs) binding both cells and Ad,[16] and polycations to neutralize repulsions between target cell membranes and viral particles.[17–22] For instance, substitution of the Ad5 knob with the Ad3 knob enhanced initial virus-cell interaction, implicating the importance of knob domains in the adenoviral life cycle and the feasibility of replacement of the knob for improving transduction of Ad5 vectors.[12] Alternatively, it is reasonable to hypothesize that the Ad5 tropism can be expanded by temporarily replacing the native Ad5 knob with other Ad serotype knobs, such as the Ad37 knob, which can bind to CD46 and a branched hexasaccharide in the GD1a on the cell surface.[23,24] This transient modification without Ad5 genome alteration would be beneficial for retaining essential recombinant virus properties, such as replication rates and transgene expression of Ad5 vectors.

In cancer treatment, oncolytic viruses (OVs) are promising in killing tumor cells, but the rapid clearance from the blood circulation prevents them from reaching the tumor microenvironment. Therefore,

Received 20 February 2020; accepted 28 May 2020;
https://doi.org/10.1016/j.omtm.2020.06.010.

Correspondence: Anja Ehrhardt, Chair for Virology and Microbiology, Center for Biomedical Education and Research (ZBAF), Department of Human Medicine, Faculty of Health, Witten/Herdecke University, Stockumerstrasse 10, 58453 Witten, Germany.
E-mail: anja.ehrhardt@uni-wh.de

cell carriers are emerging for the delivery of OVs.[25–28] In the case that novel OVs display efficient infection rates into target tumor cells but not cell carriers, the temporarily replaced knob in chimeric OVs might enhance the OV transduction into cell carriers. After release of the oncolytic agent from these cell carriers in tumor sites, the novel OV could infect target tumor cells efficiently. In this study, we explored natural killer (NK) cell derivatives (NK-92 cells[29]) as cell carriers for oncolytic Ad. NK cells are innate immune cells and play an essential role in the first-line defense against pathogen invasion and malignant transformation. NK-92 cells and chimeric antigen receptor-modified NK-92 cells were explored in the clinic and were shown to fulfill strong antitumor effects.[30]

Based on an engineered human Ad library consisting of a broad range of wild-type Ad with measurable marker genes generated in our laboratory,[31] we transduced diverse cell lines and then performed luciferase reporter assays to measure transduction efficiencies. Among all of the Ad candidates, Ad37 showed highest transduction efficiencies into NK-92, HS 578T, and A549 cells when directly compared to the Ad5 vector. Therefore, we constructed HEK293-Ad5/37-microRNA (miRNA) cells stably expressing fused Ad5/37 and a miRNA against the Ad5 knob, which were utilized for the production of chimeric Ad5/37 vectors comprising a chimeric Ad5/37 capsid and an Ad5 genome. We used this system to package the OV Ad5-human telomerase reverse transcriptase (hTERT), which can subsequently transduce NK-92 cells serving as virus carrier cells. After delivery of this OV to tumor cells by NK-92 cells, the OV can be released to destroy tumor cells. In conclusion, this method for temporary assembly of chimeric virus knobs has important implications in terms of ameliorating the implementation of virus vectors in gene therapy and cancer treatment.

RESULTS

High-Throughput Screening of Ad Tropisms

We previously constructed an Ad library in which all adenoviral vectors express TurboGFP and NanoLuc luciferase as reporters (Figure S1).[31] To analyze the Ad tropism *in vitro*, we applied these reporter-labeled adenoviral vectors at different virus particle (vp) numbers/cell to infect cell lines deriving from diverse organs. Transduction efficiencies evaluated by luciferase reporter assays were standardized by comparison with the commonly used Ad5 vector. We found that Ad5 resulted in higher transduction efficiencies compared to other adenoviral vector types in hepatocellular carcinoma Huh7 and Hep3B cell lines, the T cell leukemia Jurkat cell line, as well as bone osteosarcoma U-2 OS and Saos-2 cell lines (Figure 1A). However, Ad37 displayed up to 50-fold higher transduction efficiencies compared to Ad5 in the NK cell-derived malignant non-Hodgkin's lymphoma cell line NK-92, human primary periodontal ligament fibroblast (PdLF) cells, and the mammary gland/breast carcinoma cell line Hs 578T (Figure 1B). We also transduced hepatocellular carcinoma HepG2 cells, the retina cell line ARPE-19, and lung-derived A549 cells and found that differences in reporter gene expression levels between the tested adenoviral vectors were comparably low (Figure 1C).

The Expression of Ad Receptors CD46, CAR, and GD1a on the Cell Surface

To explore the reason for different Ad infection tropisms, we measured the expression levels of established Ad receptors on the cells mentioned above using flow cytometry. Analyzed receptors were CD46, known as a receptor for species B Ad, CAR, known to bind Ad5 and other Ad types, and the Ad37 receptor, which was shown to be GD1a ganglioside. Looking at the percentage of receptor-positive cells, the results revealed that CD46 was widely expressed on all tested cells, while expression of GD1a was relatively low on the majority of analyzed cells (Figures 2A–2C; Figure S2). The expression of CD46 was higher than CAR on NK-92, PdLF, and Hs 578T cells, which could explain that the transduction efficiencies of Ad37 were higher than those for Ad5 when analyzing these two cell lines (Figure 2B; Figure S2). The comparably low expression levels of GD1a on NK-92, PdLF, and Hs 578T cells further support the notion that CD46 could mediate sialic acid-independent transduction of Ad37 into cells.[24] Note that the mean fluorescence intensity (MFI) for CD46 was relatively high in Huh7, Hep3B, U-2 OS, Hs 578T, A549, ARPE-19, and HepG2 cells, while the MFI for CAR-positive populations (Hep3B, ARPE-19, and HepG2 cells) was stronger than in the other investigated cell lines (Figure 2D). The MFI measuring the GD1a expression levels was low in all investigated cell lines (Figure 2D).

Generation and Characterization of HEK293-Ad5/37 Cells Stably Expressing Chimeric Ad5/37 Fiber

Our results revealed that NK-92 cells are efficiently transduced by Ad37 but refractory to infection with Ad5 and that HS 578 cells showed a similar infection pattern with both viruses. Due to the attachment of the Ad37 receptor-recognizing knob domain to a branched hexasaccharide in the GD1a,[23] we attempted to replace the Ad5 knob with the Ad37 knob to increase the transduction of Ad5 vectors into cells that are efficiently transduced by Ad37 but poorly transduced by Ad5. Since the Ad5 vector possesses several advantages compared to other Ad vector types (e.g., high titer production and in-depth characterization of biological features), retaining the Ad5 vector properties and genome is necessary for its widespread application.

Therefore, we designed a method for a temporary knob protein switch in the Ad5 vector capsid schematically shown in Figure 3A. We based this technology on a cell line stably expressing a fusion protein consisting of the Ad5 shaft-tail and Ad37 knob. Since HEK293 cells are commonly used for Ad5 vector production, we stably transfected these cells, resulting in the cell line HEK293-Ad5/37. Subsequently, we utilized regular Ad5 vectors to transduce these cells for production of chimeric Ad5/37 vectors. To achieve this aim, we first constructed a biscistronic expression plasmid consisting of a fused Ad5 shaft-tail and Ad37 knob-encoding sequence linked to an internal ribosome entry site (IRES) and the selection marker neomycin/kanamycin (NeoR/KanR) (Figure 3B). Before constructing stable cell lines, we detected abundant CAR expression on the surface of HEK293 cells using flow cytometry, supporting the transduction of Ad5 vectors into

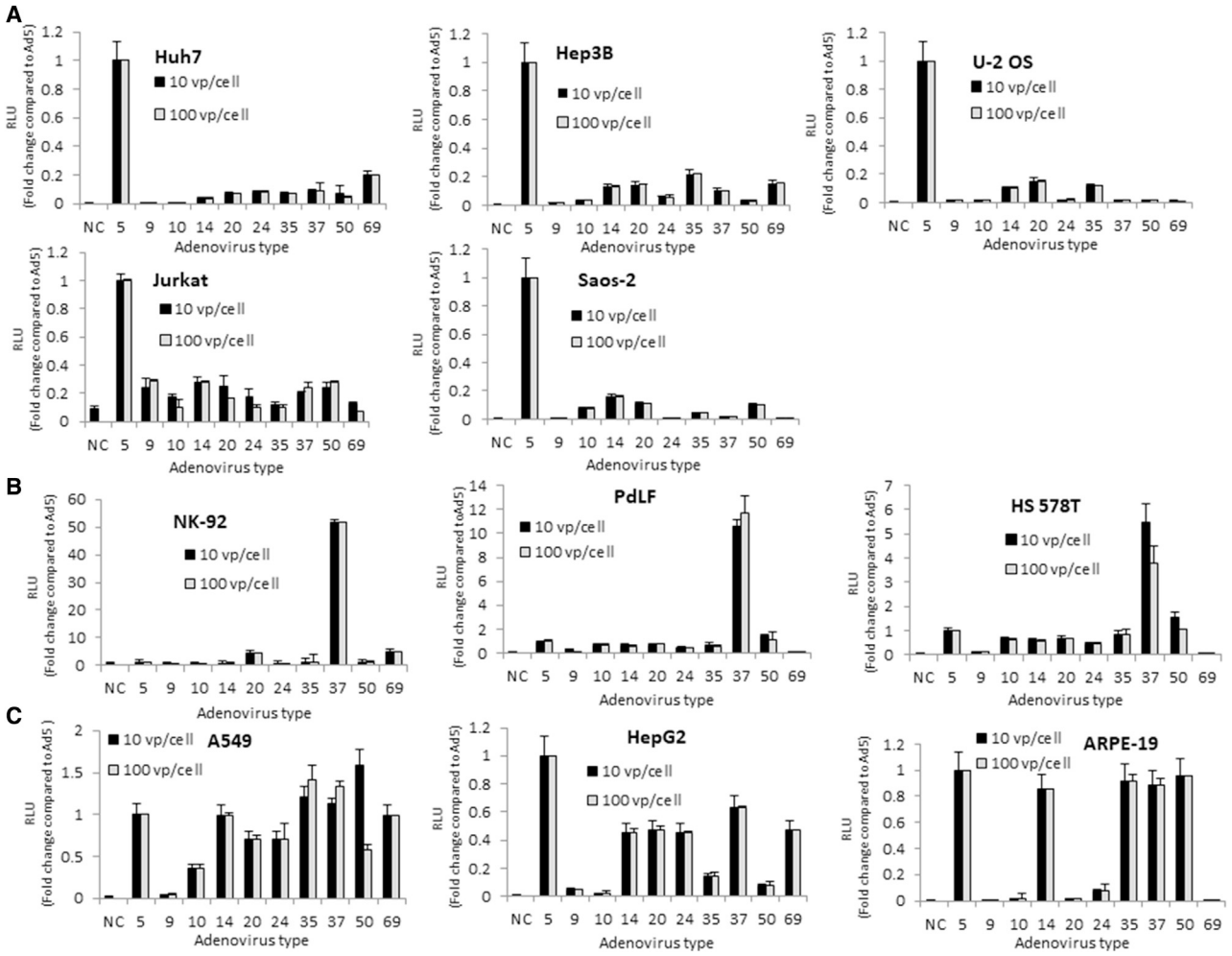

Figure 1. Screening of the Adenovirus (Ad) Tropisms in Various Human Cell Lines

Human Ad types encoding TurboGFP and NanoLuc luciferase reporters were screened and are indicated as numbers on the x axis. DNA sequences contained in the adenoviral vectors are displayed in Figure S1. Luciferase expression was measured 26 h post-infection. Values were compared to the commonly used Ad type 5 (Ad5) and indicated as fold change. (A) Huh7, Hep3B, U-2 OS, Jurkat, and Saos-2 cells were infected and luciferase expression levels measured. (B) Luciferase expression levels after infection of NK-92, PdLF, and HS 578T cells. (C) Screening of HepG2, ARPE-19, and A549 cells. In all cell lines, error bars represent mean ± SD (n = 3). GFP, green fluorescence protein; RLU, relative light units; vp, viral particles; NC, negative control. All data are from experiments performed in triplicates. Error bars represent mean ± SD (n = 3).

HEK293 cells (Figure S3). HEK293 cell lines were transfected with this expression plasmid, and cell clones were selected using G418 for 3 weeks. Then, single-cell clones were picked and cultured in 24-well plates. Subsequently, whole genomic DNA was extracted, and stable cell clones were verified for positive integration events of the fused Ad5/37 transgene via Sanger sequencing (Figure S4). For the production of chimeric Ad5/37 vectors, we transduced the HEK293-Ad5/37 cells with Ad5 vectors applying 20 vp/cell. After viral amplification for 48 h, viruses were purified using cesium chloride (CsCl) density gradient centrifugation. Next, we measured transduction efficiencies of the replication-competent chimeric Ad5/37 vectors in NK-92, HS 578T, and A549 cells and infected them at 10 and 100 vp/cell. Transduction efficiencies were detected through luciferase reporter gene expression levels, and the results revealed that chimeric Ad5/37 vector-transduced cells showed increased (up to 3-fold in NK-92 cells) luciferase reporter signals compared to Ad5 vector-transduced cells (Figure 3C). Therefore, the luciferase reporter assay indicated that the Ad37 knob in chimeric Ad5/37 vectors promoted Ad5/37 vector entry in cells poorly transduced with Ad5.

Generation and Characterization of Cells Expressing the Chimeric Fiber and a miRNA Directed against the Ad5 Fiber

In the Ad5/37 assembly process in HEK293-Ad5/37, both chimeric Ad5/37 fiber encoded by the HEK293 cells and the natural Ad5 fiber encoded by the Ad5 genome could be assembled to Ad capsids protruding from the Ad5 penton base. Here, we speculated that the

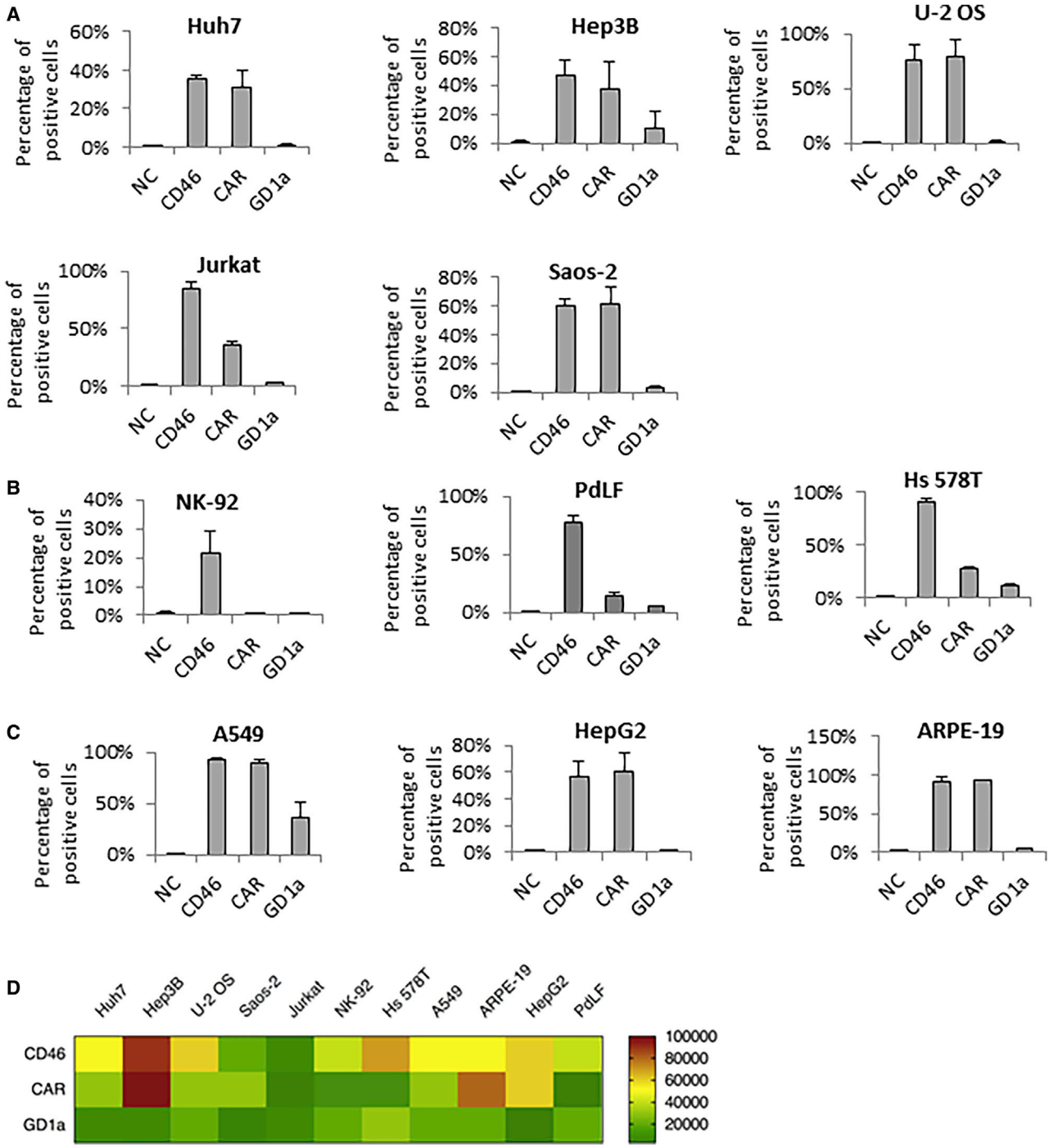

Figure 2. Measurement of Adenovirus (Ad) Receptor Expression on the Cell Surface

Flow cytometric analysis was performed for analyzing the expression levels of CD46, CAR, and GD1a. Quantitation of the percentages of positive cells for different Ad receptors is shown. (A) Huh7, Hep3B, U-2 OS, Jurkat, and Saos-2 cells were analyzed for receptor expression. (B) CD46, CAR, and GD1a receptor expression on NK-92, PdLF, and HS 578T cells. (C) Screening of HepG2, ARPE-19, and A549 cells. All data are from experiments performed in triplicates. Error bars represent mean ± SD (n = 3). (D) Mean fluorescence intensity (MFI) displayed as a heatmap of the Ad receptors CD46, CAR, and GD1a. All measured cell lines and receptors (CD46, CAR and GD1a) are summarized. A color code is used to display the intensity of the MFI.

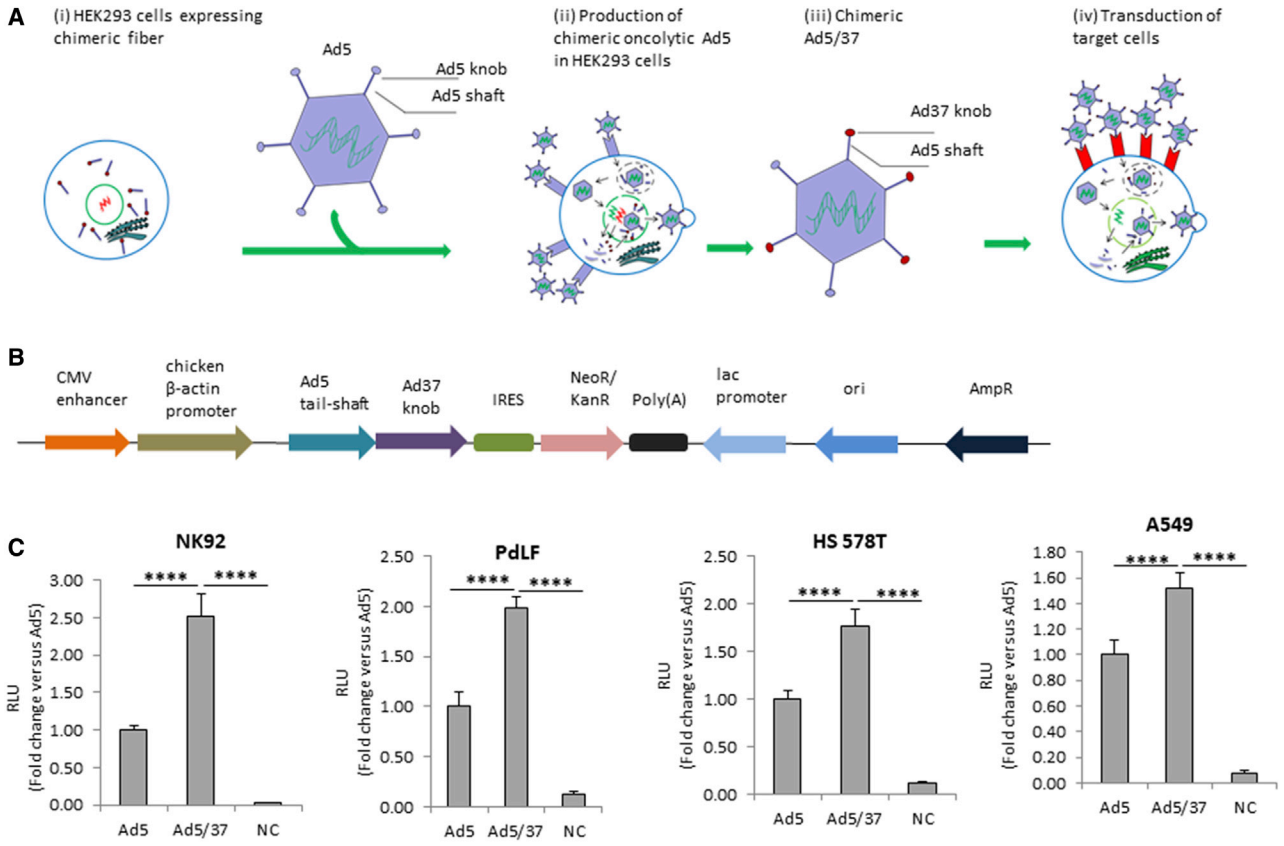

Figure 3. Characterization of HEK293-Ad5/37 Cells Stably Expressing Chimeric Ad5/37 Fiber

(A) Workflow for production of the chimeric Ad5/37 vector. After infection of target cells with the Ad5/37 vector, only the Ad5 genome is introduced into the target cells. (B) Displayed is a schematic diagram of the plasmid expressing fused Ad5/37 fiber. The fused Ad5/37 fiber consists of the Ad5 shaft-tail and Ad37 knob, the internal ribosome entry site (IRES), and the stable cell line selection marker neomycin/kanamycin-resistant element (NeoR/KanR). (C) RLU of cells transduced with chimeric Ad5/37 vectors. NK-92, PdLF, HS 578T, and A549 cells were transduced with chimeric Ad5/37, wild-type Ad5, or negative control (NC, no virus transduction). All data from experiments were performed in triplicates. Error bars represent mean ± SD (n = 3). ****$p < 0.0001$.

natural Ad5 fiber reduced the production of chimeric Ad5/37 vectors in HEK293-Ad5/37 cells. To diminish the interference of natural Ad5 fiber and increase the production of chimeric Ad5/37 vectors, it was reasonable to restrict the expression of natural Ad5 fiber. Therefore, we attempted to utilize a miRNA transcription unit to knock down Ad5 fiber but not Ad5/37 fiber and constructed HEK293 cells stably expressing both the chimeric Ad5/37 fiber and miRNA against the Ad5 knob (HEK293-Ad5/37-miRNA cells). In order to achieve this goal, we designed five plasmids expressing miRNAs (miRNA-1 to miRNA-5) binding to different positions of the Ad5 knob RNA (Figure 4A; Table S1). We transfected these five miRNA-expressing vectors into the HEK293-Ad5/37 cells and selected stable cell clones using blasticidin for 2 weeks. Subsequently, we cultured single-cell clones of each miRNA expression cassette, measured miRNA copy numbers using qPCR (Figure S5) and verified positive integration via Sanger sequencing (data not shown). Before utilizing HEK293-Ad5/37-miRNA cells for Ad5/37 vector production, we measured knockdown efficiencies of the respective miRNAs using a reporter vector that encoded Ad5 fiber protein fused with GFP (Ad5-GFP) (Figure 4B). We transfected the five HEK293-Ad5/37 cells expressing miRNA with the Ad5-GFP vector and measured the GFP fluorescence intensity. The results suggested that HEK293-Ad5/37 cells expressing miRNA-2 presented more efficient knockdown of Ad5 fiber compared with other HEK293-Ad5/37 cells expressing miRNA (Figures 4C and 4D). To explore the effect of miRNA-2 on HEK293 cell proliferation, we analyzed the cell viability of HEK293-Ad5/37 cells and HEK293-Ad5/37 cells expressing miRNA-2 using a Cell Counting Kit-8 (CCK-8) viability assay. The results showed that there is no significant difference between HEK293-Ad5/37 and HEK293-Ad5/37-miRNA cells (Figure S6), indicating that the Ad5 knob-interfering miRNA-2 had no influence on HEK293 cell proliferation. To explore the level of expression of the Ad5/37 fusion protein within the engineered HEK293-Ad5/37-miRNA cells, we compared it to the levels normally observed during Ad5 infection in HEK293 cells. Western blot analyses revealed that HEK293-Ad5/37-miRNA cells express the fused Ad5/37 fiber when compared to uninfected cells and HEK293 cells infected with Ad5 (Figure 4E). Then, we transduced HEK293 and the HEK293-Ad5/37-miRNA cells with Ad5 and purified the obtained

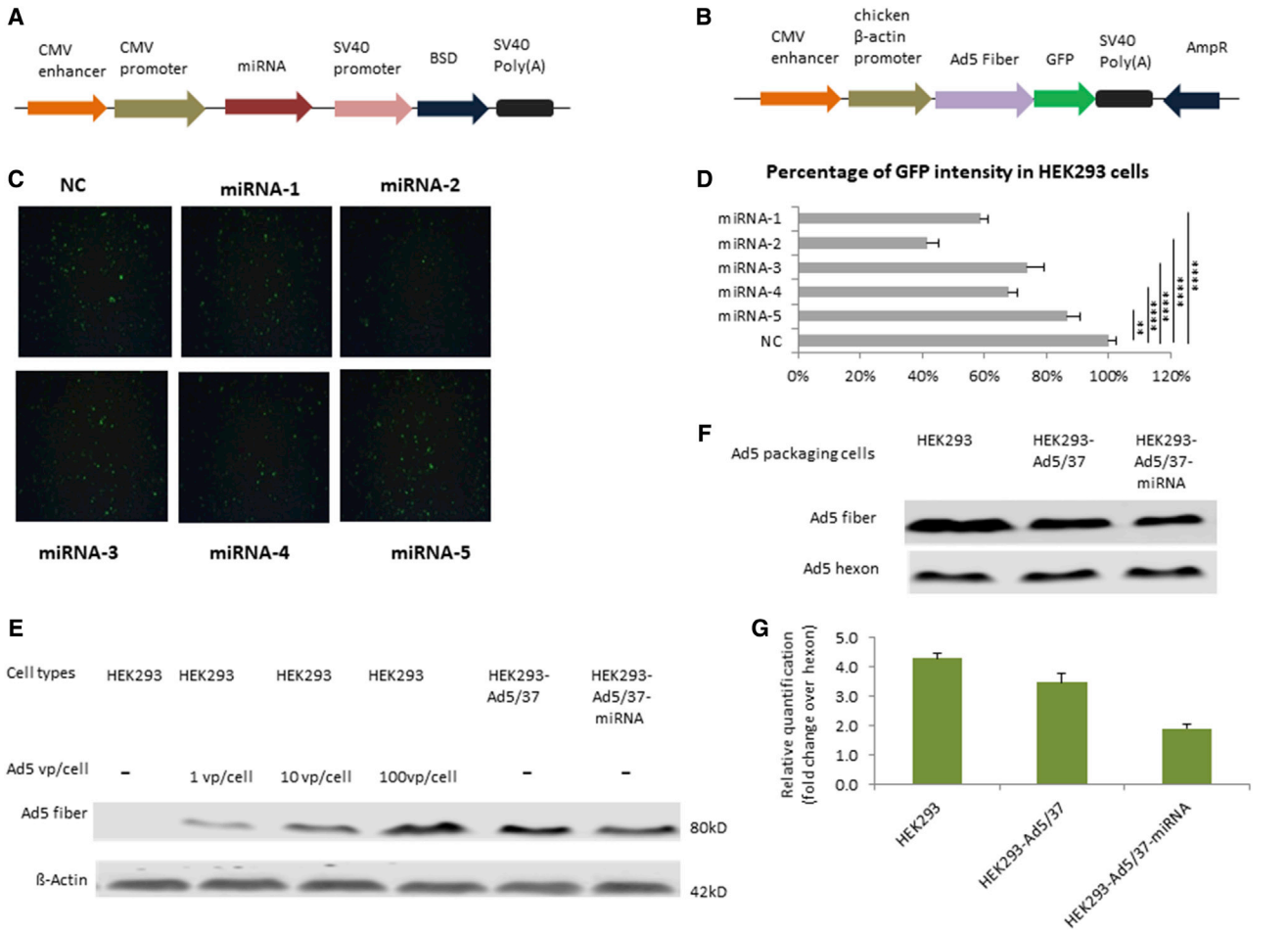

Figure 4. Construction of the HEK293-Ad5/37-miRNA Cell Line

(A) Schematic diagram of the vector expressing a miRNA binding to different positions of the Ad5 knob. BSD, blasticidin; SmR, streptomycin resistance. (B) Schematic diagram of vector-encoding Ad5 fiber proteins fused with GFP. AmpR, ampicillin resistance. (C) Fluorescence images of miRNA-expressing HEK293-Ad5/37-miRNA cells transduced with an Ad5-GFP vector. Data are from a representative experiment. NC, negative control, HEK293 cells. (D) The GFP intensity of the HEK293-Ad5/37-miRNA cells transduced with the Ad5-GFP vector is shown. (E) Western blot analysis detecting the Ad5/37 fusion protein in the engineered cells (HEK293-Ad5/37 and HEK293-Ad5/37-miRNA). As a negative control, parental HEK293 cells were used, and as a positive control, Ad5-infected HEK293 cells were analyzed. (F) Western blot analysis investigating the level of chimeric fiber protein incorporation into virions. Virions produced in HEK293, HEK293-Ad5/37, and HEK293-Ad5/37-miRNA cells were analyzed. (G) Western blot band intensity was quantified using the ImageJ software, and the relative quantification of Ad5 fiber was defined as the fold change compared to Ad5 hexon, respectively. All data are from experiments performed in triplicates. Error bars represent mean ± SD (n = 3). $^{**}p < 0.01$, $^{****}p < 0.0001$.

viral vectors. Next, we measured the level of chimeric and unmodified Ad5 fiber protein incorporation in virions using western blot analyses. The results showed that Ad5/37 amplified in HEK293-Ad5/37-miRNA cells presented less Ad5 fiber protein than did Ad5 amplified in HEK293 cells (Figures 4F and 4G), indicating the Ad5 knob was to a certain extent replaced by the Ad37 knob. Therefore, we applied HEK293-Ad5/37 cells expressing miRNA-2 (HEK293-Ad5/37-miRNA) to produce chimeric Ad5/37 vectors.

Chimeric Ad5/37 Vectors Displayed Higher Transduction Efficiencies into Target Cells

To determine transduction efficiencies of chimeric Ad5/37 vectors produced by HEK293-Ad5/37-miRNA cells, we transduced the HEK293-Ad5/37-miRNA cells with Ad5 vectors applying 20 vp/cell and purified chimeric Ad5/37 vectors using CsCl density gradient centrifugation at 48 h post-transduction. Next, we conducted qPCR to analyze the genomic DNA of the Ad5 vector in cells at 3 h post-transduction and found that chimeric Ad5/37 vector particles resulted in 15-fold, 3-fold, and 4-fold higher transduction efficiencies in NK-92, HS 578T, and A549 cells, respectively, when directly compared to the Ad5 transduced counterparts (Figure 5A).

Next, we conducted transduction experiments in NK-92, HS 578T, and A549 cell lines using different virus dosages of the chimeric Ad5/37 vector and measured luciferase expression levels at 24 h post-transduction. The chimeric Ad5/37 vector-transduced NK-92,

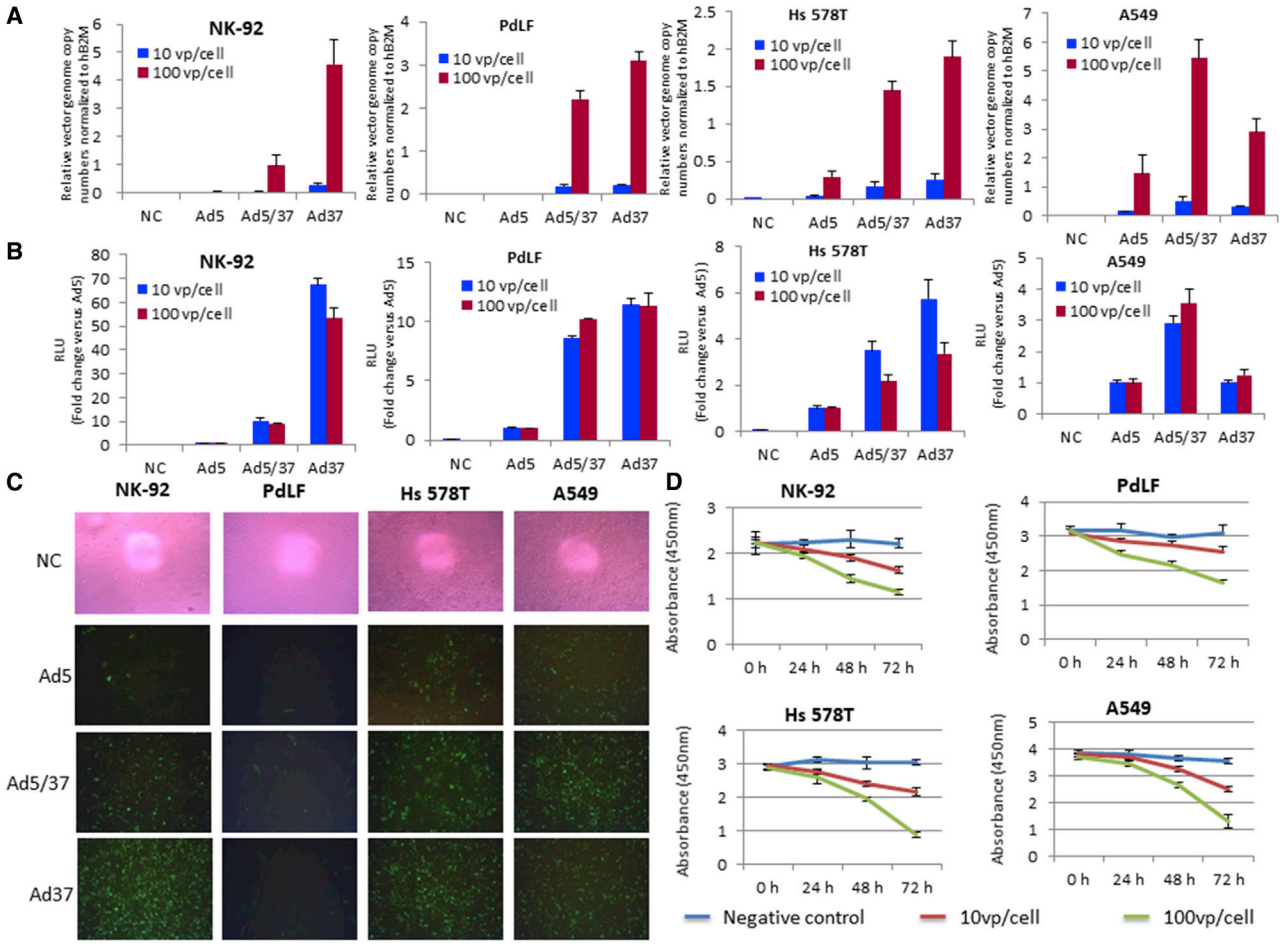

Figure 5. Transduction Efficiencies of Transiently Modified Chimeric Ad5/37 Vectors into NK-92, PdLF, Hs 578T, and A549 Cells

(A) Quantification of vector genome copy numbers after infection with the chimeric Ad5/37 vector, Ad5, and Ad37 encoding TurboGFP and NanoLuc.[31] Total genomic DNA was isolated 3 h post-transduction, and then quantitative PCR (qPCR) was conducted for detecting the Ad5 vector genome. (B) RLU of luciferase expression in cells transduced with the chimeric Ad5/37 vector, Ad5, and Ad37. (C) Fluorescence images of the cells transduced with the chimeric Ad5/37 vectors, Ad5, and Ad37. Data are from one representative experiment. (D) CCK-8 viability assay of cells transduced with the chimeric Ad5/37 vector at different virus dosages. All experiments were performed in triplicates. Error bars represent mean ± SD (n = 3).

HS 578T, and A549 cells showed 10-fold, 3.5-fold, and 4-fold increased luciferase signals compared to their Ad5 vector-transduced counterparts, respectively (Figure 5B).

To further investigate tropism of the chimeric Ad5/37 fiber vector, we employed fluorescent microscopy at 72 h post-transduction with the chimeric Ad5/37 vector after infection with 100 vp/cell. The percentage of NK-92 cells expressing GFP remarkably increased when cells were transduced with the chimeric Ad5/37 vector (Figure 5C). The GFP fluorescence intensity assays in NK-92, HS 578T, A549 and PdLF cells were in concordance with results showing that Ad5/37 vector-transduced cells revealed stronger reporter gene signals than did Ad5 vector-transduced cells (Figure S7). Due to the fact that the replication of Ad in host cells might influence their viability, we further conducted a colorimetric CCK-8 viability assay. We observed that the viability of chimeric Ad5/37 vector-transduced NK-92, HS 578T, and A549 cells was reduced over time in a dose-dependent manner (Figure 5D). These results suggested that the miRNA in the HEK293-Ad5/37-miRNA cells promoted the production of the chimeric Ad5/37 vectors and resulted in vectors with enhanced transduction efficiencies compared to Ad5 entry into host cells, allowing for higher transgene expression.

Chimeric Capsid-Modified Ad5/37 Vectors Improved NK-92 Delivery of an Oncolytic Ad5

OVs are genetically engineered viruses to selectively replicate in and subsequently kill tumor cells. The tumor-specific oncolytic Ad5 vector containing the tumor-specific hTERT (Ad5-hTERT) provides a relatively safe strategy allowing the development of clinical concepts for tumor treatment.[32,33] However, the rapid clearance of OVs from the circulation reduces their ability to reach tumor sites. Therefore, cells carriers provide an attractive option for delivery of OVs

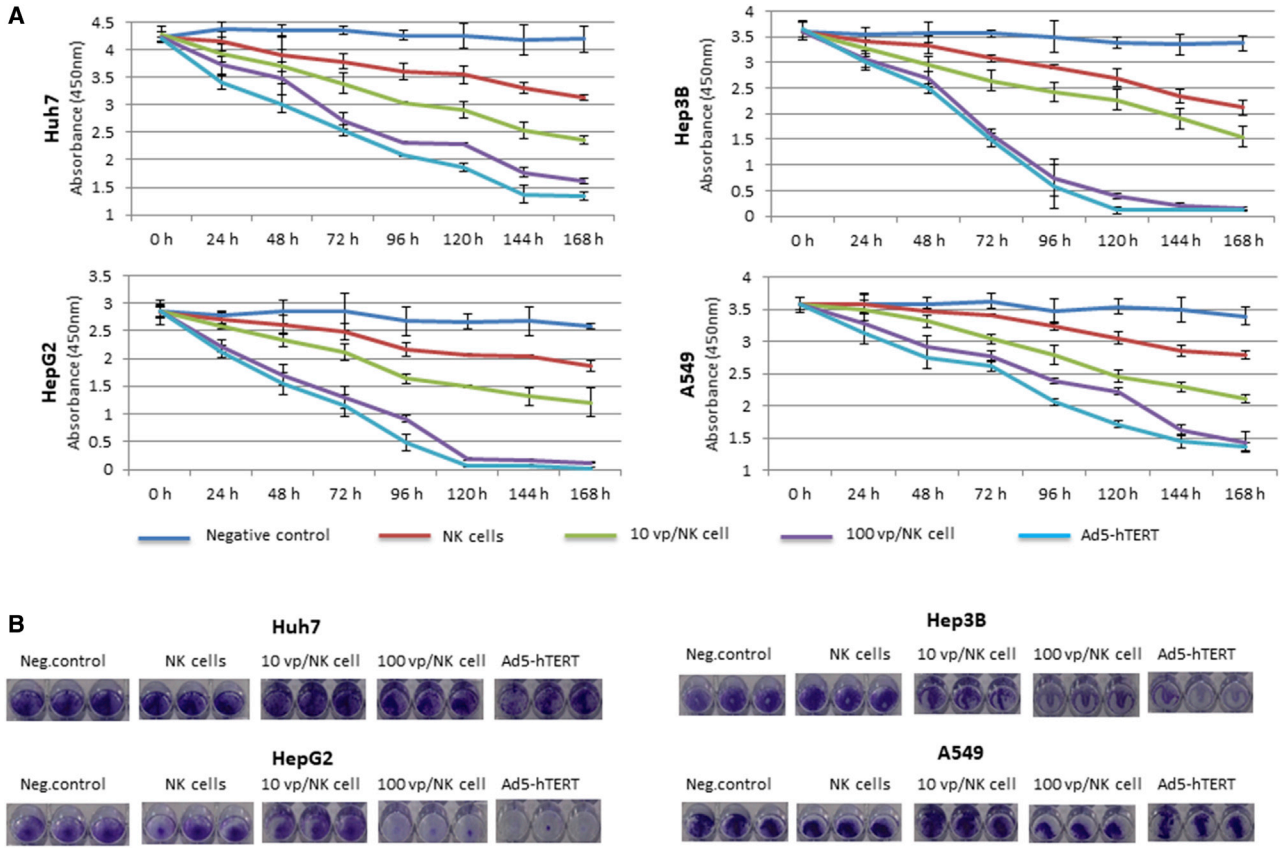

Figure 6. Delivery of Oncolytic Ad5 into Tumor Cells Using NK-92 Carrier Cells Transduced with the Chimeric Oncolytic Ad5/37 Vector

The oncolytic Ad5/37 vector used in this study is based on the oncolytic virus Ad5-hTERT. (A and B) CCK-8 viability assay (A) and oncolytic assay (B) of cells incubated with NK-92 carrier cells carrying the chimeric oncolytic Ad5/37 vector. Negative control, tumor cells; NK cells, tumor cells incubated with NK cells; 10 vp/NK cell and 100 vp/NK cell, tumor cells incubated with NK cells transduced with chimeric Ad5/37 vector at 10 vp/NK cell and 100 vp/NK cell; Ad5-hTERT, tumor cells transduced with the oncolytic Ad5 vector at 100 vp/cell. The effector (NK-92)-to-target (tumor cells) ratio was 10:1. All data are from experiments performed in triplicates. Error bars represent mean ± SD (n = 3).

potentially improving cancer treatment.[25–28] The only cell line that has been infused into patients with advanced tumors with clinical benefit and minimal side effects (ClinicalTrials.gov: NCT00900809 and NCT00990717)[34,35] were NK-92 cells. Therefore, we speculated that these cells have great potential for carrying OVs to the respective tumor site. However, the low infection rate of Ad5 into NK-92 carrier hinders NK-92 cells to carry oncolytic Ad5 into tumor sites. Since the efficacy of treatment depends on delivering sufficient amounts of oncolytic Ad5 into tumor sites through carrier cells, improvement of oncolytic Ad5 transduction into NK-92 carrier cells is essential. Therefore, we aimed to engineer a chimeric oncolytic Ad5-hTERT vector carrying an Ad37-derived knob protein on the virion surface. Using this strategy, we set up to generate NK-92 cells efficiently carrying oncolytic Ad5-hTERT vectors to tumor cells *in vitro*.

To achieve this goal, we infected the HEK293-Ad5/37-miRNA producer cells with the oncolytic Ad5-hTERT vector applying 20 vp/cell and purified the chimeric Ad5/37-hTERT virus using CsCl density gradient centrifugation. Subsequently, we incubated NK-92 cells with the Ad5/37-hTERT vector (NK-Ad5/37-hTERT) for 4 h and then washed these NK-92 cells for incubation with tumor cells. To test the efficacy of these tools, the CCK-8 assay was conducted for the determination of cell viability. The results showed that Huh7, Hep3B, HepG2, and A549 cells incubated with the NK-Ad5/37-hTERT exhibited lower viability compared to the negative control and cells incubated with untreated NK-92 cells. Particularly, Hep3B and HepG2 cells, which received the Ad5-hTERT vector via the NK-92 cell carrier infected with 100 vp/cell of the chimeric Ad5/37-hTERT vector, showed comparable viability compared to the group solely receiving the Ad5-hTERT vector (Figure 6A). Therefore, the oncolytic activity was comparable for both strategies independent of whether the OV was directly delivered to tumor cells or by indirect delivery using a cell carrier. To further evaluate the tumor-killing effects of this method, we performed crystal violent staining for the abovementioned groups based on cell killing. In contrast to experiments performed in Huh7 and A549 cells, Hep3B, HepG2, and A549 cells incubated with the NK-Ad5/37-hTERT system (100 vp/NK cell) were more effectively destroyed as shown by methylene

blue staining (Figure 6B). These results were consistent with the results of the CCK-8 assay.

DISCUSSION

Adenoviral vectors possess diverse advantages for clinical applications. In this study, we aimed at developing a technology to change the adenoviral vector tropism without vector genome alterations. We found that the widely used Ad5 vector demonstrated higher transduction efficiencies in various cell lines. However, in NK-92, Hs 578T, and A549 cells, the Ad37 vector displayed up to 50-fold higher or comparable transduction rates (Figure 1). The underlying mechanism could be the Ad receptor distribution on the cell surface. The flow cytometry data supported the importance of adenoviral cellular receptors in efficient adenoviral vector transduction. The poor transduction of Ad5 into NK-92, HS 578T, and A549 cells was supported by the data that these cells lack abundant expression of CAR. Note that although the percentage of CAR-positive A549 cells was relatively high, the MFI was relatively low.

It was previously shown that the Ad37 knob can bind to $\alpha(2\rightarrow3)$-linked sialic acid (2,3-SA) for cell entry, including A549 cells.[36,37] Moreover, the presence of 2,3-SA of the GD1a ganglioside on the cell surface might be the underlying cause that the Ad37 knob can bind to GD1a. This is consistent with our data that revealed that 36.6% of A549 cells were positive for GD1a (Figure 2B). However, it was shown that Ad37 can also transduce cells, which showed poor GD1a expression on the cell surface. The possible reason for this phenomenon could be that another Ad receptor mediates cell entry such as CD46. The Ad37 fiber knob could attach to cells through initial interaction with CD46 in a calcium-dependent and 2,3-SA-independent manner.[24,38] Meanwhile, Ad37 demonstrated efficient transduction of NK-92 cells, which lack high expressions of CD46 and GD1a. This phenomenon might lie on the reason that Ad37 has the ability to transduce NK-92 cells with other unknown receptors. In contrast, the Ad5 fiber knob lacks the ability to bind to the extracellular domain of CD46, but it can use CAR as a primary receptor. Although the Ad37 knob contains binding sites to CAR, it is unable for Ad37 to use CAR efficiently for cell entry, because the inflexible fiber restricts its attachment to CAR at the cell surface.[39,40] Interestingly, installation of the Ad37 knob onto the long and flexible Ad5 shaft allowed for pseudotyped Ad5/37 virus attachment to cells and infection.[39] However, artificial extension of the Ad5 shaft could inhibit infection into CAR-positive cells without the influence of knob-CAR interaction.[41]

The Ad fiber is a trimeric protein containing a globular knob on a long thin shaft, and the trimerization is crucial in the assembly of the capsid and its attachment to cellular receptors.[42] The trimerization signal is located within the knob region,[43,44] and therefore capsid assembly may have been disturbed by replacing the fiber knob in an Ad5 virion. However, our data in the present study and the study by Wu et al.[39] proved that the installation of an Ad37 knob into the Ad5 shaft reserves the function of Ad5 fiber.

A previous study introduced a cell line expressing fiber protein derived from Ad3.[45] In this approach, the producer cell stably expressed a chimeric fiber with the Ad3 fiber knob and the Ad5 fiber shaft. However, in this approach a genetically modified Ad5 genome was used that lacked the fiber-coding sequence. Besides the fact that viral DNA encodes heritable information essential for virus replication, it also contributes to the capsid strength and integrity.[2] Therefore, radical genome modifications might decrease virion stability.[46,47] In addition, in the case of delivering OVs to tumor sites by carrier cells, tumor cells and carrier cells might show different infection efficiencies for OVs. Therefore, it can be assumed that the genome-modified OVs lack the ability to simultaneously show high infection efficiencies for tumor cells and carrier cells, while our temporary modification strategy could address this challenge.

In contrast, for our approach an unmodified Ad5 genome can be used. Besides stably expressing the chimeric fiber protein, we also used a miRNA approach to downregulate the wild-type Ad5 fiber protein expression on the mRNA level. miRNA directs the sequence-specific degradation of mRNA through RNA interference (RNAi), which can also be mediated by short synthetic two 21- to 23-mer nt RNA duplexes.[48–51] Unlike gene scissors, miRNA interferes with mRNA expression in the cytoplasm without influencing host genomes in the nucleus. Importantly, approximately one copy of the integrated miRNA transcription unit was sufficient for high-titer vector production. Our results also proved that the chimeric Ad5/37 vector produced in HEK293-Ad5/37-miRNA cells displayed higher transduction rates than did recombinant viruses derived from HEK293-Ad5/37 cells.

With respect to virotherapy, for cells displaying higher transduction of Ad37 than Ad5 vectors, such as NK-92, HS 578T, and A549 cells, the permanent replacement of the Ad5 knob with the Ad37 knob through the alteration of the domain-encoding region would be superior to transient substitution. However, for cells with high CAR expression, preserving the knob in Ad5 vectors is crucial for retaining infectivity of oncolytic Ad5 vectors into these cells, because the knob is a primary mediator of Ad5 binding to CAR on the tumor cell surface.[4,5,52] There are various strategies to broaden the tropism and to increase transduction efficiency of Ad5-based vectors,[53] including the incorporation of a targeting peptide into the fiber knob domain (the HI loop and/or C terminus). Other options include pseudotyping Ad5 vectors by placing the knob domain derived from an alternate serotype, which binds to receptors other than CAR, or combining serotype chimers with peptide ligands. Expression of two separate fibers with distinct receptor-binding capabilities on the same viral particle and fiber xenotyping by replacing the knob and shaft domains of wild-type Ad5 fiber protein with the fibritin trimerization domain of T4 bacteriophage[54,55] or $\sigma1$ attachment protein of reovirus[56] may also be feasible.

Furthermore, the combination of OV-based therapy and emerging immunotherapies are attractive strategies for tumor treatment. The method wherein OVs bind to the surface of their cell carrier has

been used for a long time, but the surface-bound virus is exposed to neutralizing Abs and complement.[27,57] However, internal packaging of the virus in cell carriers can overcome these obstacles. Until now, a variety of cell types, including cytokine-induced killer cells (CIKs),[58] dendritic cells,[26,27] and T cells,[59] have been used as OV carriers in tumor treatments. Compared with peripheral T and NK cells, NK-92 cells have the following advantages in clinical treatment: a continuously growing cell line consisting of "pure" (100%) activated NK cells, expansion in serum-free medium without feeders but only interleukin (IL)-2, higher transfection efficiency, and the possibility to have NK-92 cryopreserved and expanded upon thawing (before infusion).[60] The transient modification of the oncolytic Ad5-hTERT vector allowed infection of NK-92 cells, which then deliver the OV to tumor cells, but these tumor cells presented different oncolysis states. CAR is widely expressed on various tumor cells at different levels,[61] and it plays crucial roles in Ad5 infection.[62] HepG2 and Hep3B cells demonstrated stronger expression of CAR (Figure S2) and showed more pronounced oncolysis than did Huh7 and A549 cells in the case of incubation with NK-92 cells carrying the transiently modified Ad5/37-hTERT vector (Figure 6B). The NK-92 carrier cells would facilitate OVs to *circumvent* the binding to normal cells for instance in the blood and improve the on-target delivery. Importantly, it is necessary to retain virus transduction into tumor cells while improving its transduction into cell carriers. Therefore, we used the Ad37 knob to improve the oncolytic Ad5-hTERT entry into NK-92. We think that this presents an encouraging strategy to employ NK-92 cells to deliver Ad5-hTERT into tumor sites not only *in vitro* but also *in vivo*.

In the future, a xenograft model is needed for exploring NK-92-mediated delivery of oncolytic Ad5-hTERT to tumor sites. In the tumor cell line or tumor patient-derived xenografts (PDXs), we could analyze the trafficking of NK-92 cells into tumors, the influence of NK-92 carrier cells on tumor microenvironment, the quantity of viruses released from NK-92 cells, and the tumor inhibition efficacy of Ad5-hTERT. Based on the results from the *in vitro* experiments, research in a xenograft model is under consideration and will be conducted in further studies.

In conclusion, the temporary assembly of chimeric Ad5/37 fiber in the Ad5 vector improved its transduction into desired target cells. This method provides a promising tool to broaden the transduction tropism of a virus vector without modifying its virus genome.

MATERIALS AND METHODS

Cell Culture

All human cell lines were available in our laboratory, with the exception of Hep3B and HepG2 cells, which were donated by Barbara Sitek (Ruhr University Bochum). NK-92 cells were obtained from Winfried Wels (Institute for Tumor Biology and Experimental Therapy, Frankfurt, Germany). Huh7 cells were cultured in Dulbecco's modified Eagle's medium (DMEM, PAN-Biotech) supplemented with non-essential amino acids (NEAAs, PAN-Biotech). Human PdLF, Hs 578T, A549, ARPE-19, and HEK293 cells were maintained in DMEM and Hep3B cells were maintained in Eagle's minimum essential medium (MEM, PAN-Biotech). U-2 OS and Saos-2 cells were cultured in McCoy's 5A medium modified (PAN-Biotech), whereas Jurkat and HepG2 cells were cultured in RPMI 1640 (PAN-Biotech). NK-92 cells were cultured in DMEM containing 2 mM L-glutamine (PAN-Biotech), 1 mM sodium pyruvate, and 100 U/mL IL-2 (Promega). All of the abovementioned media were supplemented with 10% fetal bovine serum (FBS, GE Healthcare) and 1% penicillin/streptomycin (PAN-Biotech). Cells were maintained at 37°C in a humid atmosphere containing 5% CO_2.

Flow Cytometry Analyses for Ad Receptor Detection

The measurement of Ad receptor expression on the cell surface was conducted using flow cytometry analyzes. We used 0.2×10^6 cells for each panel and stained with monoclonal Abs. For measurements of CD46 and CAR expressions, the Abs phycoerythrin (PE)-CD46 (Invitrogen) and PE-CAR (Sino Biological) were used. The staining procedure was performed in the dark at room temperature (20°C–25°C) for 30 min. For measurement of GD1a expressions on the cell surface, cells were stained with primary mouse anti-GD1a ganglioside antibody (Sigma-Aldrich) and then the secondary rat anti-mouse IgG1 antibody (Invitrogen) was used for staining in the dark at room temperature (20°C–25°C) for 30 min. After staining, the cells were washed twice with phosphate-buffered saline and detected using a CytoFLEX flow cytometer (Beckman Coulter). The data were analyzed using CytExpert software (Beckman Coulter).

Construction of Plasmids

For the construction of the Ad5/37-IRES-Neo/Kan plasmid, based on the Ad5 and Ad37 genomes, we generated the Ad5/37 chimeric fiber DNA sequence containing the Ad5 shaft-tail and Ad37 knob through overlap PCR. The following primers were used (note that the AfeI and NotI-HF restriction sites are underlined): forward primer binding to the N′-Ad5 shaft-tail-encoding region, 5′-ATTAGCGCTCAGAT GAAGCGCGCAAGACCG-3′; reverse primer binding to the C′-Ad37 knob-encoding region, 5′-GAT GCG GCC GCT CAT TCT TGG GCA ATA TAG GAG-3′. The bridge primers were as follows: forward primer binding to the N′-Ad37 knob-encoding region, 5′-AAG CTA ACT TTG TGG ACC ACA CCA GAC ACA TCT CCA AAC TGC ACA ATT-3′; reverse primer binding to C′-Ad5 shaft-tail-encoding region, 5′-TGG TGT GGT CCA CAA AGT TAG CTT ATC ATT-3′. Briefly, the extension PCR of the PCR fragments containing the overlapping fragments were performed using a PrimeSTAR Max DNA polymerase kit (Takara). PCR fragments were cleaned up by the my-Budget Double Pure Kit (Bio-Budget Technologies) and applied as a template for the subsequent overlap PCR. The overlap PCR ran 15 PCR cycles without primer followed by the purification PCR, which ran for 15–20 cycles with the end primers, resulting in the fused Ad5/37-encoding region. The fused Ad5/37-encoding region was gel extracted using the my-Budget Double Pure Kit, and then inserted into the pJET1.2/blunt cloning vector for the construction of pJET1.2-Ad5/37. After validation by Sanger sequencing, the pJET1.2-Ad5/37 was digested with AfeI (NEB) and NotI-HF (NEB), gel extracted, and inserted upstream of the IRES-Neo/KanR

sequences in the plasmid pCMV-IRES-Neo/KanR. The final plasmid, Ad5/37-IRES-Neo/KanR, contained the cytomegalovirus (CMV) enhancer and CMV promoter.

Construction of the Ad5 knob-miRNA-expressing plasmid was conducted according to the description of the BLOCK-iT polymerase II (Pol II) miR RNAi expression vector kit provided by Invitrogen. The five chosen miRNAs interfering with Ad5 knob expression used in this study are not naturally occurring miRNAs existing in cells. These miRNAs are designer miRNAs related to the BLOCK-iT Pol II miR RNAi expression vector kit provided by Invitrogen. The BLOCK-iT Pol II miR RNAi technology uses miRNA expression vectors that allow expression of knockdown cassettes driven by RNA Pol II promoters in mammalian cells. The expression vectors use a modified miR-155 precursor stem-loop and an endogenous murine flanking sequence to express synthetic miRNAs complementary to target RNAs.[1] To design miRNA sequences (single-stranded DNA oligonucleotides) using the BLOCK-iT RNAi Designer (https://rnaidesigner.thermofisher.com/rnaiexpress/design.do), we chose the miR RNAi in "target design options" and entered the Ad5 knob nucleotide sequence. Then, we selected the minimum and maximum G/C percentage of 35% and 55%, respectively. Next, we clicked "RNAi design" to design the miR RNAi molecules for cloning into Invitrogen's vector pcDNA6.2-GW/miR. Finally, 10 top scoring miR RNAi sequences of 21 bp were reported according to their knockdown probability. From the 10 miR RNAi sequence candidates, we chose 5, targeting different regions of the Ad5 knob (Figure S8; Table S1). Subsequently, we generate the top and bottom oligonucleotide sequences for every miRNA sequence. The top oligonucleotide sequence combines the following elements in the following order: (1) 5′TGCTG, (2) reverse complement of the sense target sequence, (3) GTTTTGGCCACTGACTGAC (terminal loop), (4) nucleotides 1–8 (5′-3′) of the sense target sequence, and (5) nucleotides 11–21 (5′-3′) of the sense target sequence. The bottom oligonucleotide sequences contained the following elements: (1) the sequence 5′CCTG, (2) the reverse complement of the top sequence excluding 5′TGCTG, and (3) 3′C. After that, we annealed the top and bottom oligonucleotides and cloned the double-stranded oligonucleotide into the pcDNA6.2-GW/miR vector. The miRNA vector was transfected into cells to interfere with the respective target mRNA.

For the construction of the Ad5 fiber-GFP plasmid, we first got the Ad5 fiber-encoding region through PCR using the Ad5 genome as a template. The primers were as follows (note that the XbaI and MluI restriction sites are underlined): forward primer binding to the N′-Ad5 fiber-encoding region, 5′-GGC TCT AGA ATG AAG CGC GCA AGA CCG-3′; reverse primer binding to the C′-Ad5 fiber-encoding region, 5′-TAC CAC GCG TTC TTG GGC AAT GTA TGA AAA AGT GT-3′. The Ad5 fiber-encoding region was gel extracted and then inserted into the pJET1.2/blunt cloning vector for the construction of pJET1.2-Ad5 fiber. After validation by Sanger sequencing, the pJET1.2-Ad5 fiber was digested with XbaI (NEB) and MluI (NEB), gel extracted, and inserted in front of GFP-encoding region in pCMV-GFP plasmid for the construction of the Ad5 fiber-GFP plasmid with the CMV enhancer and CMV promoter.

Generation of Stable Cell Lines

For the generation of HEK293-Ad5/37 stable cells, HEK293 cells were transfected with the Ad5/37-IRES-Neo/KanR plasmid using a calcium phosphate transfection protocol. 3 days later, cells were split, serially diluted, and transferred into 10-cm dishes. 24 h later, the media were replaced with selective media containing 550 mg/mL G418 (Carl Roth, Germany). The selection was maintained for 3 weeks with media changes performed every 3 days to eliminate dead cells. The HEK293-Ad5/37 stable cell genome was extracted, and the Ad5/37 fragment was PCR amplified and sequenced.

For the generation of HEK293-Ad5/37-miRNA stable cells, the HEK293-Ad5/37 stable cells were transfected with Ad5 knob-miRNA vectors using a calcium phosphate transfection protocol. 3 days later, cells were split, serially diluted, and transferred into 10-cm dishes. 24 hours later, the media was replaced with selective media containing 500 mg/mL blasticidin (Invitrogen). The selection was maintained for 2 weeks with media changes performed every 3 days to eliminate dead cells. The HEK293-Ad5/37-miRNA stable cell genome was extracted, and the Ad5/37 fragment was PCR amplified and sequenced.

Production of the Chimeric Ad5/37 and Ad5/37-hTERT Viral Vectors

The Ad5 vector is from our Ad library and it expresses TurboGFP and NanoLuc luciferase as reporters as described previously.[31] We received the oncolytic Ad5-hTERT vector from Florian Kühnel (Medical School Hannover).[63] The Ad5 and Ad5-hTERT vectors were transduced into HEK293-Ad5/37 or HEK293-Ad5/37-miRNA cells and, 48 h post-transduction, the chimeric Ad5/37 and Ad5/37-hTERT viral vectors were purified using CsCl density gradient centrifugation. The total vp and infectious units of the purified vectors were measured by qPCR. Except for experiments shown in Figure 6, for which we used Ad5-hTERT, the replication-competent Ad5 virus expressing TurboGFP and NanoLuc[31] was used.

Transduction of Cells with the Ad5/37 Vector

The infection efficiency of the chimeric replication-competent Ad5 and Ad5-hTERT vectors containing Ad37 knob into NK-92 cells was measured by qPCR. NK-92 cells were grown to confluency in 24-well tissue culture plates and were infected with different vp per cell. At 3 h post-infection, cell genomes were extracted and the Ad5 infection efficiency was measured using qPCR. At the same time, the cytopathic effect (CPE) was checked to detect the time span that Ad5-hTERT will remain in NK-92 carrier cells.

Western Blot Analysis

For the detection of Ad fiber expression in HEK293 and HEK293-Ad5/37-miRNA cells, the amount of total protein was determined by applying a bicinchoninic acid (BCA) protein assay kit (Thermo Fisher Scientific). 100 μg of total protein was run in 10% SDS-polyacrylamide gel and transferred onto polyvinylidene fluoride

(PVDF) membrane (Invitrogen) using semi-dry transfer. The membrane was blocked using 5% milk/Tris-buffered saline plus Tween 20 (TBST) and incubated with the primary antibody against Ad5 fiber (Lab Vision, MS-1027-PO). As an internal control, β-actin was assessed using a β-actin antibody (Abcam). To detect Ad5 hexon we used an Ad5 hexon antibody (Abcam, ab24240).

To measure the level of fiber protein incorporation in virions, 10e8 viral particles were run on a SDS-polyacrylamide gel (4%) and subsequently transferred onto a PVDF membrane (Invitrogen). After blocking, the membrane was incubated with primary antibody against Ad5 fiber, and as a reference Ad5 hexon was detected from purified virus derived from HEK293 and HEK293-Ad5/37-miRNA cells.

After washing with TBST, membranes were incubated with the IRDye 800CW secondary Abs (LI-COR Biosciences). The Odyssey CLx imaging system (LI-COR Biosciences) was used to visualize the bands. ImageJ was used to quantify western blot band intensity.

Ad5 Genome Detection

For the detection of Ad5 genomes, total genomic DNA of Ad5/37-transduced cells was prepared for qPCR. The primers used for the PCR reaction binding to the late 3 (L3) region of the Ad5 genome were as follows: forward, 5′-GAG TTG GCA CCC CTA TTC GA-3′; reverse, 5′-ATG CCA CAT CCG TTG ACT TG-3′. The endogenous human β_2-microglobulin gene (hB2M) gene was used for normalization. The hB2M primers were as follows: forward, 5′-TGCTGTCTCCATGTTTGATGTATCT-3′; reverse, 5′-TCTCTG CTCCCCACCTCTAAGT-3′. Each gene was amplified in triplicates and the average threshold cycle (Ct) was used for calculation. The relative fold changes in genome copy numbers were calculated using the comparative Ct ($2^{-\Delta Ct}$) method.

Cell Viability Assay

Cell viability was measured using a CCK-8 assay (Sigma-Aldrich) according to the manufacturer's instructions. NK-92, Hs 578T, and A549 cells were grown in 24-well plates and transduced with the Ad5/37 vector at 10 and 100 vp/cell. 24, 48, and 72 h post-transduction, cells in a total volume of 400 μL of medium were incubated with 100 μL of CCK-8 assay solution in each well for 2 h. Tumor cells mixed with the Ad5/37-infected NK-92 carrier cells were incubated for 4 h and then washed. Then, Huh7, Hep3B, HepG2, and A549 cells cultured in 24-well plates were incubated with the virus-treated NK-92 cells for 24, 48, 72, 96, 120, 144, and 168 h. Subsequently, the cells in 400 μL of medium were incubated with 100 μL of CCK-8 assay solution in each well for 2 h. The absorbance values at 450 nm were then measured using an Infinite F Plex plate reader (Tecan). Assays were repeated three times.

Crystal Violet Staining

NK-92 cell carriers were infected with the chimeric Ad5/37-hTERT vectors, which were then added to the pre-seeded tumor cells (Huh7, Hep3B, HepG2, and A549 cells). The CPE was checked daily until at least one plate showed CPE or until a maximum of 10 days. The tumor cells were fixed with 3.7% formaldehyde and then stained with crystal violet solution for detecting the density of live cells. The crystal violet staining was performed in 24-well plates.

Statistical Analyses

For multiple comparisons, statistical comparison was analyzed using the one-way analysis of variance (ANOVA) test (alpha = 0.05) followed by the Bonferroni test using GraphPad Prism (version 8.3.1, GraphPad, San Diego, CA, USA). Statistical results were reported as means ± SD. $p < 0.05$ was considered statistically significant. All results were from experiments performed in triplicates.

SUPPLEMENTAL INFORMATION

Supplemental Information can be found online at https://doi.org/10.1016/j.omtm.2020.06.010.

AUTHOR CONTRIBUTIONS

J.G. designed the research, conducted experiments, analyzed the data, and wrote the manuscript. W.Z. constructed adenovirus vectors. K.M. and O.B. participated in flow cytometry assays and oncolytic assays. F.L. revised the manuscript. A.E. designed the research and revised the manuscript. All authors approved the final version of the manuscript.

CONFLICTS OF INTEREST

The authors declare no competing interests.

ACKNOWLEDGMENTS

NK-92 cells were kindly provided by Winfried Wels at the University of Frankfurt (Frankfurt, Germany). PdLF cells were donated by Jingchao Hu at the Capital Medical University School of Stomatology (Beijing, China). The oncolytic Ad5-hTERT vector was a generous gift of Florian Kühnel (Medical School Hannover, Hannover, Germany). This work was supported by the China Scholarship Council to J.G. (CSC201506010255), internal research funding of the Witten/Herdecke University to J.G. (IFF 2019-21), and by the DFG to A.E. (EH 192/5-3).

REFERENCES

1. Hage, E., Gerd Liebert, U., Bergs, S., Ganzenmueller, T., and Heim, A. (2015). Human mastadenovirus type 70: a novel, multiple recombinant species D mastadenovirus isolated from diarrhoeal faeces of a haematopoietic stem cell transplantation recipient. J. Gen. Virol. *96*, 2734–2742.

2. Robinson, C.M., Singh, G., Lee, J.Y., Dehghan, S., Rajaiya, J., Liu, E.B., Yousuf, M.A., Betensky, R.A., Jones, M.S., Dyer, D.W., et al. (2013). Molecular evolution of human adenoviruses. Sci. Rep. *3*, 1812.

3. Lopez-Gordo, E., Doszpoly, A., Duffy, M.R., Coughlan, L., Bradshaw, A.C., White, K.M., Denby, L., Nicklin, S.A., and Baker, A.H. (2017). Defining a novel role for the coxsackievirus and adenovirus receptor in human adenovirus serotype 5 transduction *in vitro* in the presence of mouse serum. J. Virol. *91*, e02487-16.

4. Bergelson, J.M., Cunningham, J.A., Droguett, G., Kurt-Jones, E.A., Krithivas, A., Hong, J.S., Horwitz, M.S., Crowell, R.L., and Finberg, R.W. (1997). Isolation of a common receptor for coxsackie B viruses and adenoviruses 2 and 5. Science *275*, 1320–1323.

5. Tomko, R.P., Xu, R., and Philipson, L. (1997). HCAR and MCAR: the human and mouse cellular receptors for subgroup C adenoviruses and group B coxsackieviruses. Proc. Natl. Acad. Sci. USA *94*, 33C52–3356.

6. Leopold, P.L., and Crystal, R.G. (2007). Intracellular trafficking of adenovirus: many means to many ends. Adv. Drug Deliv. Rev. *59*, 810–821.

7. Brunetti-Pierri, N., Palmer, D.J., Beaudet, A.L., Carey, K.D., Finegold, M., and Ng, P. (2004). Acute toxicity after high-dose systemic injection of helper-dependent adenoviral vectors into nonhuman primates. Hum. Gene Ther. *15*, 35–46.

8. Yei, S., Mittereder, N., Wert, S., Whitsett, J.A., Wilmott, R.W., and Trapnell, B.C. (1994). In vivo evaluation of the safety of adenovirus-mediated transfer of the human cystic fibrosis transmembrane conductance regulator cDNA to the lung. Hum. Gene Ther. *5*, 731–744.

9. Thomas, C.E., Birkett, D., Anozie, I., Castro, M.G., and Lowenstein, P.R. (2001). Acute direct adenoviral vector cytotoxicity and chronic, but not acute, inflammatory responses correlate with decreased vector-mediated transgene expression in the brain. Mol. Ther. *3*, 36–46.

10. Parker, A.L., White, K.M., Lavery, C.A., Custers, J., Waddington, S.N., and Baker, A.H. (2013). Pseudotyping the adenovirus serotype 5 capsid with both the fibre and penton of serotype 35 enhances vascular smooth muscle cell transduction. Gene Ther. *20*, 1158–1164.

11. Von Seggern, D.J., Aguilar, E., Kinder, K., Fleck, S.K., Gonzalez Armas, J.C., Stevenson, S.C., Ghazal, P., Nemerow, G.R., and Friedlander, M. (2003). In vivo transduction of photoreceptors or ciliary body by intravitreal injection of pseudotyped adenoviral vectors. Mol. Ther. *7*, 27–34.

12. Kawakami, Y., Li, H., Lam, J.T., Krasnykh, V., Curiel, D.T., and Blackwell, J.L. (2003). Substitution of the adenovirus serotype 5 knob with a serotype 3 knob enhances multiple steps in virus replication. Cancer Res. *63*, 1262–1269.

13. Capasso, C., Garofalo, M., Hirvinen, M., and Cerullo, V. (2014). The evolution of adenoviral vectors through genetic and chemical surface modifications. Viruses *6*, 832–855.

14. Matsui, H., Sakurai, F., Katayama, K., Yamaguchi, T., Okamoto, S., Takahira, K., Tachibana, M., Nakagawa, S., and Mizuguchi, H. (2012). A hexon-specific PEGylated adenovirus vector utilizing blood coagulation factor X. Biomaterials *33*, 3743–3755.

15. Suzuki-Kouyama, E., Katayama, K., Sakurai, F., Yamaguchi, T., Kurachi, S., Kawabata, K., Nakagawa, S., and Mizuguchi, H. (2011). Hexon-specific PEGylated adenovirus vectors utilizing avidin-biotin interaction. Biomaterials *32*, 1724–1730.

16. Wickham, T.J., Lee, G.M., Titus, J.A., Sconocchia, G., Bakács, T., Kovesdi, I., and Segal, D.M. (1997). Targeted adenovirus-mediated gene delivery to T cells via CD3. J. Virol. *71*, 7663–7669.

17. Fasbender, A., Zabner, J., Chillón, M., Moninger, T.O., Puga, A.P., Davidson, B.L., and Welsh, M.J. (1997). Complexes of adenovirus with polycationic polymers and cationic lipids increase the efficiency of gene transfer in vitro and in vivo. J. Biol. Chem. *272*, 6479–6489.

18. Matthews, C., Jenkins, G., Hilfinger, J., and Davidson, B. (1999). Poly-L-lysine improves gene transfer with adenovirus formulated in PLGA microspheres. Gene Ther. *6*, 1558–1564.

19. Gao, L., Wagner, E., Cotten, M., Agarwal, S., Harris, C., Rømer, M., Miller, L., Hu, P.C., and Curiel, D. (1993). Direct in vivo gene transfer to airway epithelium employing adenovirus-polylysine-DNA complexes. Hum. Gene Ther. *4*, 17–24.

20. Arcasoy, S.M., Latoche, J.D., Gondor, M., Pitt, B.R., and Pilewski, J.M. (1997). Polycations increase the efficiency of adenovirus-mediated gene transfer to epithelial and endothelial cells in vitro. Gene Ther. *4*, 32–38.

21. Toyoda, K., Nakane, H., and Heistad, D.D. (2001). Cationic polymer and lipids augment adenovirus-mediated gene transfer to cerebral arteries in vivo. J. Cereb. Blood Flow Metab. *21*, 1125–1131.

22. Buo, A.M., Williams, M.S., Kerr, J.P., and Stains, J.P. (2016). A cost-effective method to enhance adenoviral transduction of primary murine osteoblasts and bone marrow stromal cells. Bone Res. *4*, 16021.

23. Nilsson, E.C., Storm, R.J., Bauer, J., Johansson, S.M., Lookene, A., Ångström, J., Hedenström, M., Eriksson, T.L., Frängsmyr, L., Rinaldi, S., et al. (2011). The GD1a glycan is a cellular receptor for adenoviruses causing epidemic keratoconjunctivitis. Nat. Med. *17*, 105–109.

24. Wu, E., Fernandez, J., Fleck, S.K., Von Seggern, D.J., Huang, S., and Nemerow, G.R. (2001). A 50-kDa membrane protein mediates sialic acid-independent binding and infection of conjunctival cells by adenovirus type 37. Virology *279*, 78–89.

25. Yang, Z., Zhang, Q., Xu, K., Shan, J., Shen, J., Liu, L., Xu, Y., Xia, F., Bie, P., Zhang, X., et al. (2012). Combined therapy with cytokine-induced killer cells and oncolytic adenovirus expressing IL-12 induce enhanced antitumor activity in liver tumor model. PLoS ONE *7*, e44802.

26. Jennings, V.A., Ilett, E.J., Scott, K.J., West, E.J., Vile, R., Pandha, H., Harrington, K., Young, A., Hall, G.D., Coffey, M., et al. (2014). Lymphokine-activated killer and dendritic cell carriage enhances oncolytic reovirus therapy for ovarian cancer by overcoming antibody neutralization in ascites. Int. J. Cancer *134*, 1091–1101.

27. Ilett, E.J., Prestwich, R.J., Kottke, T., Errington, F., Thompson, J.M., Harrington, K.J., Pandha, H.S., Coffey, M., Selby, P.J., Vile, R.G., and Melcher, A.A. (2009). Dendritic cells and T cells deliver oncolytic reovirus for tumour killing despite pre-existing anti-viral immunity. Gene Ther. *16*, 689–699.

28. Muthana, M., Rodrigues, S., Chen, Y.Y., Welford, A., Hughes, R., Tazzyman, S., Essand, M., Morrow, F., and Lewis, C.E. (2013). Macrophage delivery of an oncolytic virus abolishes tumor regrowth and metastasis after chemotherapy or irradiation. Cancer Res. *73*, 490–495.

29. Gong, J.H., Maki, G., and Klingemann, H.G. (1994). Characterization of a human cell line (NK-92) with phenotypical and functional characteristics of activated natural killer cells. Leukemia *8*, 652–658.

30. Zhang, C., Oberoi, P., Oelsner, S., Waldmann, A., Lindner, A., Tonn, T., and Wels, W.S. (2017). Chimeric antigen receptor-engineered NK-92 cells: an off-the-shelf cellular therapeutic for targeted elimination of cancer cells and induction of protective antitumor immunity. Front. Immunol. *8*, 533.

31. Zhang, W., Fu, J., Liu, J., Wang, H., Schiwon, M., Janz, S., Schaffarczyk, L., von der Goltz, L., Ehrke-Schulz, E., Dörner, J., et al. (2017). An engineered virus library as a resource for the spectrum-wide exploration of virus and vector diversity. Cell Rep. *19*, 1698–1709.

32. Yu, B., Zhang, Y., Zhan, Y., Zha, X., Wu, Y., Zhang, X., Dong, Q., Kong, W., and Yu, X. (2011). Co-expression of herpes simplex virus thymidine kinase and Escherichia coli nitroreductase by an hTERT-driven adenovirus vector in breast cancer cells results in additive anti-tumor effects. Oncol. Rep. *26*, 255–264.

33. Lin, J., Zeng, D., He, H., Tan, G., Lan, Y., Jiang, F., and Sheng, S. (2017). Gene therapy for human ovarian cancer cells using efficient expression of Fas gene combined with γδT cells. Mol. Med. Rep. *16*, 3791–3798.

34. Arai, S., Meagher, R., Swearingen, M., Myint, H., Rich, E., Martinson, J., and Klingemann, H. (2008). Infusion of the allogeneic cell line NK-92 in patients with advanced renal cell cancer or melanoma: a phase I trial. Cytotherapy *10*, 625–632.

35. Tonn, T., Schwabe, D., Klingemann, H.G., Becker, S., Esser, R., Koehl, U., Suttorp, M., Seifried, E., Ottmann, O.G., and Bug, G. (2013). Treatment of patients with advanced cancer with the natural killer cell line NK-92. Cytotherapy *15*, 1563–1570.

36. Arnberg, N., Edlund, K., Kidd, A.H., and Wadell, G. (2000). Adenovirus type 37 uses sialic acid as a cellular receptor. J. Virol. *74*, 42–48.

37. Arnberg, N., Kidd, A.H., Edlund, K., Olfat, F., and Wadell, G. (2000). Initial interactions of subgenus D adenoviruses with A549 cellular receptors: sialic acid versus α_v integrins. J. Virol. *74*, 7691–7693.

38. Wu, E., Trauger, S.A., Pache, L., Mullen, T.M., von Seggern, D.J., Siuzdak, G., and Nemerow, G.R. (2004). Membrane cofactor protein is a receptor for adenoviruses associated with epidemic keratoconjunctivitis. J. Virol. *78*, 3897–3905.

39. Wu, E., Pache, L., Von Seggern, D.J., Mullen, T.M., Mikyas, Y., Stewart, P.L., and Nemerow, G.R. (2003). Flexibility of the adenovirus fiber is required for efficient receptor interaction. J. Virol. *77*, 7225–7235.

40. Law, L.K., and Davidson, B.L. (2005). What does it take to bind CAR? Mol. Ther. *12*, 599–609.

41. Seki, T., Dmitriev, I., Kashentseva, E., Takayama, K., Rots, M., Suzuki, K., and Curiel, D.T. (2002). Artificial extension of the adenovirus fiber shaft inhibits infectivity in coxsackievirus and adenovirus receptor-positive cell lines. J. Virol. *76*, 1100–1108.

42. Stouten, P.F., Sander, C., Ruigrok, R.W., and Cusack, S. (1992). New triple-helical model for the shaft of the adenovirus fibre. J. Mol. Biol. *226*, 1073–1084.

43. Hong, J.S., and Engler, J.A. (1996). Domains required for assembly of adenovirus type 2 fiber trimers. J. Virol. *70*, 7071–7078.

44. Novelli, A., and Boulanger, P.A. (1991). Deletion analysis of functional domains in baculovirus-expressed adenovirus type 2 fiber. Virology *185*, 365–376.

45. Von Seggern, D.J., Huang, S., Fleck, S.K., Stevenson, S.C., and Nemerow, G.R. (2000). Adenovirus vector pseudotyping in fiber-expressing cell lines: improved transduction of Epstein-Barr virus-transformed B cells. J. Virol. *74*, 354–362.

46. Saha, B., Wong, C.M., and Parks, R.J. (2014). The adenovirus genome contributes to the structural stability of the virion. Viruses *6*, 3563–3583.

47. Shayakhmetov, D.M., Li, Z.Y., Gaggar, A., Gharwan, H., Ternovoi, V., Sandig, V., and Lieber, A. (2004). Genome size and structure determine efficiency of postinternalization steps and gene transfer of capsid-modified adenovirus vectors in a cell-type-specific manner. J. Virol. *78*, 10009–10022.

48. Zamore, P.D., Tuschl, T., Sharp, P.A., and Bartel, D.P. (2000). RNAi: double-stranded RNA directs the ATP-dependent cleavage of mRNA at 21 to 23 nucleotide intervals. Cell *101*, 25–33.

49. Hammond, S.M., Bernstein, E., Beach, D., and Hannon, G.J. (2000). An RNA-directed nuclease mediates post-transcriptional gene silencing in Drosophila cells. Nature *404*, 293–296.

50. Nair, J.K., Willoughby, J.L., Chan, A., Charisse, K., Alam, M.R., Wang, Q., Hoekstra, M., Kandasamy, P., Kel'in, A.V., Milstein, S., et al. (2014). Multivalent *N*-acetylgalactosamine-conjugated siRNA localizes in hepatocytes and elicits robust RNAi-mediated gene silencing. J. Am. Chem. Soc. *136*, 16958–16961.

51. Ryther, R.C., Flynt, A.S., Phillips, J.A., 3rd, and Patton, J.G. (2005). siRNA therapeutics: big potential from small RNAs. Gene Ther. *12*, 5–11.

52. Santis, G., Legrand, V., Hong, S.S., Davison, E., Kirby, I., Imler, J.L., Finberg, R.W., Bergelson, J.M., Mehtali, M., and Boulanger, P. (1999). Molecular determinants of adenovirus serotype 5 fibre binding to its cellular receptor CAR. J. Gen. Virol. *80*, 1519–1527.

53. Stepanenko, A.A., and Chekhonin, V.P. (2018). Tropism and transduction of oncolytic adenovirus 5 vectors in cancer therapy: focus on fiber chimerism and mosaicism, hexon and pIX. Virus Res. *257*, 40–51.

54. Krasnykh, V., Belousova, N., Korokhov, N., Mikheeva, G., and Curiel, D.T. (2001). Genetic targeting of an adenovirus vector via replacement of the fiber protein with the phage T4 fibritin. J. Virol. *75*, 4176–4183.

55. Kim, J.W., Kane, J.R., Young, J.S., Chang, A.L., Kanojia, D., Morshed, R.A., Miska, J., Ahmed, A.U., Balyasnikova, I.V., Han, Y., et al. (2015). A genetically modified adenoviral vector with a phage display-derived peptide incorporated into fiber fibritin chimera prolongs survival in experimental glioma. Hum. Gene Ther. *26*, 635–646.

56. Mercier, G.T., Campbell, J.A., Chappell, J.D., Stehle, T., Dermody, T.S., and Barry, M.A. (2004). A chimeric adenovirus vector encoding reovirus attachment protein sigma1 targets cells expressing junctional adhesion molecule 1. Proc. Natl. Acad. Sci. USA *101*, 6188–6193.

57. Cole, C., Qiao, J., Kottke, T., Diaz, R.M., Ahmed, A., Sanchez-Perez, L., Brunn, G., Thompson, J., Chester, J., and Vile, R.G. (2005). Tumor-targeted, systemic delivery of therapeutic viral vectors using hitchhiking on antigen-specific T cells. Nat. Med. *11*, 1073–1081.

58. Sampath, P., Li, J., Hou, W., Chen, H., Bartlett, D.L., and Thorne, S.H. (2013). Crosstalk between immune cell and oncolytic vaccinia therapy enhances tumor trafficking and antitumor effects. Mol. Ther. *21*, 620–628.

59. Ong, H.T., Hasegawa, K., Dietz, A.B., Russell, S.J., and Peng, K.W. (2007). Evaluation of T cells as carriers for systemic measles virotherapy in the presence of antiviral antibodies. Gene Ther. *14*, 324–333.

60. Klingemann, H. (2014). Are natural killer cells superior CAR drivers? OncoImmunology *3*, e28147.

61. Reeh, M., Bockhorn, M., Görgens, D., Vieth, M., Hoffmann, T., Simon, R., Izbicki, J.R., Sauter, G., Schumacher, U., and Anders, M. (2013). Presence of the coxsackievirus and adenovirus receptor (CAR) in human neoplasms: a multitumour array analysis. Br. J. Cancer *109*, 1848–1858.

62. Ortiz-Zapater, E., Santis, G., and Parsons, M. (2017). CAR: a key regulator of adhesion and inflammation. Int. J. Biochem. Cell Biol. *89*, 1–5.

63. Boozari, B., Mundt, B., Woller, N., Strüver, N., Gürlevik, E., Schache, P., Kloos, A., Knocke, S., Manns, M.P., Wirth, T.C., et al. (2010). Antitumoural immunity by virus-mediated immunogenic apoptosis inhibits metastatic growth of hepatocellular carcinoma. Gut *59*, 1416–1426.